Nonlinear resonances generate large-scale convection cells in phase space

Fan Wu, Dmitri Vainchtein, and Anton Artemyev

Phys. Rev. E **99**, 020201 — Published 5 February 2019

DOI: 10.1103/PhysRevE.99.020201

Nonlinear resonances generate large-scale convection cells in the phase space

Fan Wu[1], Dmitri Vainchtein[2,3], Anton Artemyev[4,3]
[1] *Key Laboratory of Traffic Safety on Track, Ministry of Education, School of Traffic & Transportation Engineering, Central South University, Changsha 410075, Hunan, China*
[2] *Nyheim Plasma Institute, Drexel University, Camden, NJ, USA*
[3] *Space Research Institute, Moscow, Russia*
[4] *Institute of Geophysics and Planetary Physics, University of California, Los Angeles, CA, USA*
(Dated: January 11, 2019)

It is well-known that the resonance phenomena can destroy the adiabatic invariance and cause chaos and mixing. In the present paper, we show that the nonlinear wave-particle resonant interaction may do the opposite – generate large-scale coherent structures in the phase space. The combined action of the drift due to nonlinear scattering on resonance and trapping (capture) into resonance creates a convection cell-like structure, where the areas of particle acceleration and deceleration are macroscopically separated. At the same time, nonlinear scattering also creates a diffusion that cause mixing on energy levels and between the energy levels.

Convection cells and large-scale coherent structures are common in the physical space of fluid systems. However, similar structures in the phase space of Hamiltonian systems are much more rare [1–3]. In the present letter we introduce a simple system of charged particles moving in a non-uniform magnetic field in the presence of an electrostatic wave. In many plasma systems, charged particle resonant interaction with electromagnetic waves represent the only way of an efficient energy exchange between particle populations. For coherent resonant interaction particles can spend a long time within the resonance and their dynamics become much more complicated than just a diffusion in the phase space. The first study of mixing and chaos due to resonances was done by Feingold and co-workers, [4–6] who recognized that mixing is caused by the breakdown of adiabatic invariance near surfaces where the frequency of the perturbation is in resonance with the frequency of the unperturbed flow. Many example of chaotic advection and mixing in fluids in the presence of resonances can be found in [7]. Recently, the nonlinear wave-particle interaction became one of the main approaches to the quantitative description of plasma processes in magnetosphere, [8–12]. Our analysis is based on modelling charged particle motion in an effective potential generated by a combination of Lorentz forces from the background magnetic field and wave electromagnetic field. We show that particles interacting with such potentials may form large-scale convection cells in the *phase* space. The internal structure of these cells and their evolution due to particles exchange between trapped and nontrapped (transient) populations determine the wave dumping/growth, particle acceleration/deceleration, and many other important wave characteristics. In a classical problem of the nonlinear Landau damping, the trapped phase space region is assumed to be uniformly filled, and thus the events of particle trapping/escape can influence the wave dynamics [e.g., 13, 14]. In many systems, effects related to formation and evolution of large-scale structures control the primary wave dynamics and secondary wave formation [e.g., 15–18].

In the present paper we present a simple setting where the nonlinear resonance phenomena create a phase-space convection cell. We start with main equations of the wave-particle system and introduce the separation of time scales. Then we define the resonance and describe scattering at resonance and trapping (capture) into resonance at a single crossing. After that we describe the structure of the convection cell, estimate the time-scale of mixing and the period of the convection cell. Finally, we propose a kinetic Fokker-Plank-type equation that describes the leaking of particles from the cell.

Dimensionless Hamiltonian of a charged particle moving in a double-well potential in the presence of a fast wave is

$$H = \frac{1}{2}p_y^2 + U(y) + \beta \sin \chi\varphi, \qquad U(y) = \left(\alpha^2 y^2 - 1\right)^2 / 8\alpha^2, \qquad \varphi = y - ut \tag{1}$$

Here χ, u, and β are the wavenumber, the phase speed, and the amplitude of the wave, respectively. We assume that the wave is short, $\chi = 30 \gg 1$, and weak, $\beta = 0.1 \ll 1$. The other parameters are $\alpha = 0.1$ and $u = 1$. The minimum possible value of energy, $H_{min} = 0$, is at the bottom of the either of the two potential wells; $H_C = 1/(8\alpha^2) = 12.5$ is the value of energy at the potential barrier at $y = 0$. The unperturbed system is illustrated in Fig. 1. The separatrix S separates the motion inside one of the two wells from the motion in the top domain.

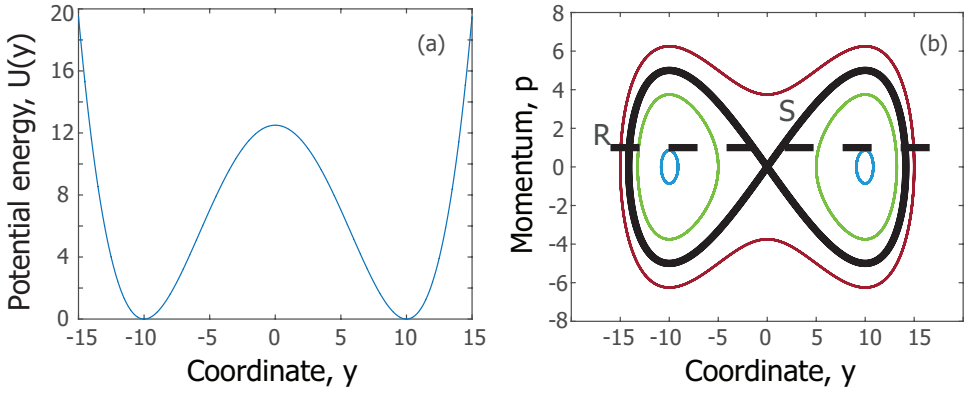

FIG. 1. The unperturbed system: (a) Profile of the potential energy; (b) Phase portrait.

The smallness of $1/\chi \ll 1$ introduces a separation of time scales: φ is fast, while (y, p_y) and H are slow. In the first approximation, we can average Hamiltonian (1) over the fast phase, which is effectively equivalent to omitting the term $\beta \sin(\chi\varphi)$ in (1): $H_{av} = p_y^2/2 + \left(\alpha^2 y^2 - 1\right)^2 / 8\alpha^2$. As H_{av} does not depend on time explicitly, it is an integral of the averaged system. In exact system (1), the value of H is approximately conserved (with the accuracy of order β) everywhere, where the separation of time scales is valid and the method of averaging works. The averaging fails when the rate of change of φ vanishes on the line called a *Resonance*: $d\varphi/dt = p_y - u = 0$ (dashed line R in

Fig. 1(b)). Dynamics of particles that intersect the resonance is drastically different from that of the particles that do not intersect it. Most particles cross the resonance twice on each period of the fast motion. There are two kinds of exceptions. Particles near the bottom of the two wells ($H < H_{min} = 0.5$) do not cross the resonance at all (two smallest circles in Fig. 1(b)); those just above the separatrix S cross the resonance four times. Every time a particle crosses a resonance, the value of energy H changes. There are two main resonance phenomena: capture (trapping) into resonance and scattering on resonance, see [e.g., 12] and references therein.

During most of the resonance crossings, the energy of a particle changes only slightly. This process is called scattering on resonance. It follows from [e.g., 12, 19] and references therein, that the change of the energy is

$$\Delta H(\xi, H) = -u\sqrt{\beta}\sqrt{2a}\int_{-\infty}^{\tilde{\varphi}_*} \frac{\cos\tilde{\varphi}\, d\tilde{\varphi}}{\sqrt{2\pi\xi + \tilde{\varphi} - a\sin\tilde{\varphi}}} \tag{2}$$

where $\tilde{\varphi} = \chi\varphi$, $a = \beta\chi/A$ and $A = A(H) = \partial U/\partial y = y_R\left(\alpha^2 y_R^2 - 1\right)/2$. The value of A is computed at the resonance crossing: $H = u^2/2 + \left(\alpha^2 y_R^2 - 1\right)^2/8\alpha^2$. In (2), $\tilde{\varphi}_*$ is the value of $\tilde{\varphi}$ at the resonance crossing, and $2\pi\xi = \tilde{\varphi}_* - a\sin\tilde{\varphi}_*$. The value of ξ is a very sensitive function of the initial conditions: even small, order β, changes in the initial conditions result in significant changes in ξ, see [e.g., 12] and references therein. For multiple consecutive scatterings, ξ can be treated as a random variable uniformly distributed on $(0, 1)$, see a numerical verification of this assumption in [20]. Correspondingly, ΔH becomes a random variable as well.

Statistical properties of ΔH depend on the value of a. The average value and the second moment of ΔH are

$$\langle\Delta H\rangle(H) = \int_0^1 \Delta H(\xi, H)\, d\xi; \quad \left\langle(\Delta H)^2\right\rangle(H) = \int_0^{2\pi} \left(\Delta H(\xi, H) - \langle\Delta H\rangle\right)^2 d\xi \tag{3}$$

It was shown in [21], that when $a > 1$, $\langle\Delta H\rangle$ is finite, and when $a < 1$, $\langle\Delta H\rangle = 0$; $\left\langle(\Delta H)^2\right\rangle$ is always finite.

Besides scattering, particles may be trapped (captured) into resonance. Trapping is possible if $a > 1$ and $da/dt > 0$ along the trajectory. In the current system, particles can be captured on the left walls in both wells. It was shown in [e.g., 12, 22, 23] that trapping can be considered as a random process. While for every given particle approaching the resonance it can be predicted will it be trapped or not (provided trapping is possible), this trapped-or-not-trapped transition is very sensitive to initial conditions. Thus, for multiple particles and multiple passages through resonance, it is reasonable to consider trapping as a probabilistic process. The method of computing the probability of trapping, $\Pi(H)$, is presented in several papers, see [e.g., 12, 24] and references therein.

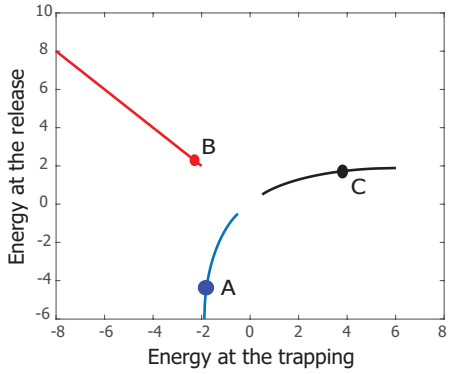

FIG. 2. Trapping (capture) into resonance: input-output function. Horizontal axis: $H\text{sign}(y)$ at the trapping, vertical axis: $H\text{sign}(y)$ at the release. Note that the energy H is multiplied by sign(y). Thus the left and the right wells corresponds to $H\text{sign}(y) < 0$, and $H\text{sign}(y) > 0$, respectively.

Once a particle is trapped into resonance, its dynamics is integrable and predictable. The trapped particles move for a while with the wave: they are transported along the resonance and then are released from resonance on the right walls. The value of the energy at the release from resonance can be computed explicitly, [e.g., 25]. The energy input-output function is presented in Fig. 2, where we used $H\text{sign}(y)$ instead of H to distinguish between the left and right wells. In the left well, for $-H < -H_{lr} \approx -2$, particles are transported to the right wall of the right well (L-R capture). From the symmetry of the potential well with respect to the axis $x = 0$, in this case the energy does not change. This trapping corresponds to the red, top left, line in Fig. 2. For $0 < H_{tr} < H_{lr}$, particles are transported to the right wall of the left well (L-L capture). In this case, the energy grows (the blue, bottom left, line in Fig. 2).

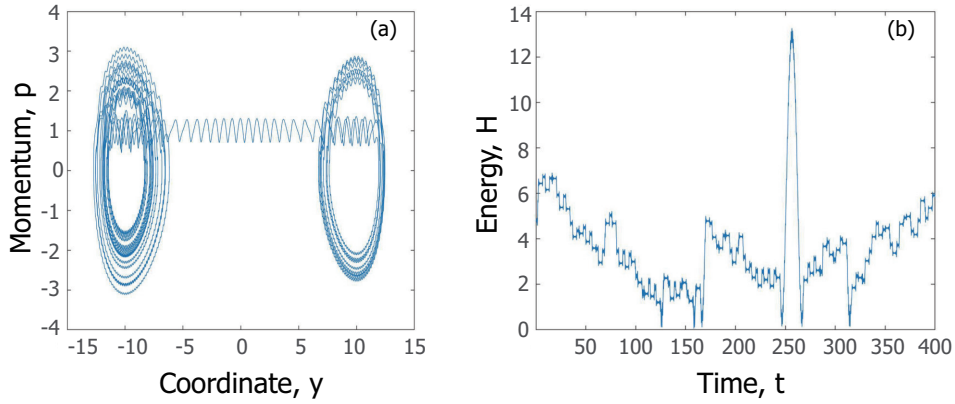

FIG. 3. Trapping (capture) into resonance. (a): Phase portrait; (b): Energy evolution.

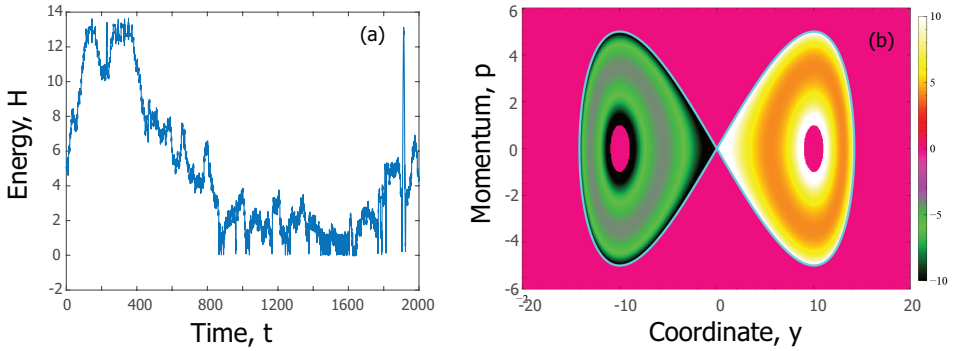

FIG. 4. Medium-time evolution: (a): trajectory of a single particle: from the right well, up to the top well, down the left well, and transfer by capture into resonance to the right well, and starting up again. (b): The average change of energy.

In the right well, all the particles captured at the left wall are transported to the right wall. The energy decays (the black, top right, line in Fig. 2).

An interval of the phase trajectory containing all three types of trapping is presented in Fig. 3. First the particle is trapped (at $t \approx 170$ in Fig. 3(b), the outer spiral in the left well in the left panel in Fig. 3(a)) in the left well and released in the left well (Point A in Fig. 2). The second time the trapping occurs at a higher value of the energy (at $t \approx 245$ in Fig. 3(b), the long spiral in Fig. 3(a)), and the particle is transported to the right well (Point B in Fig. 2). The third trapping (at $t \approx 320$ in Fig. 3(b), the outer spiral in the right well in Fig. 3(a)) move the particles from the left wall of the right well to the right wall (Point C in Fig. 2).

The medium-time behaviour of any given particle consists of the successive motion in three distinct domains: the right well, the left well, and the top domain (above the barrier). A characteristic dynamics is illustrated in Fig. 4(a). In the right well, the value of energy grows on average, resulting in the upward advection in the phase space. Then the particle enters the top domain ($t \approx 120$) where there is no drift, just a diffusion. In terms of energy, particles can go up – there is no upper bound – or down. Most of the particles spend some time in the top domain ($t \approx 120 - 400$). If they go down to the right well (e.g., $t \approx 200$), advection kicks them back to the top domain immediately. However, if a particle goes down the left well ($t \approx 400$), advection takes it down ($t \approx 400 - 900$). Near the bottom, trapping into resonance becomes possible. While the energy is not too small, above H_{lr}, trapping takes the particle from the left well to the right well: the L-R trapping. Once below H_{lr}, trapping keeps the particle inside the left well: the L-L trapping. However, the energy at the release from the L-L trapping is larger than H_{lr}. Therefore, the L-R trapping becomes possible again. The particle oscillates near the bottom of the left well undergoing the downward drift and the upward L-L trappings ($t \approx 900 - 1900$) until finally the L-R trapping occurs ($t \approx 1900$). After that the particle is transported to the right well and the whole process repeats again.

The structure of the resulting convection cell is illustrated in Fig. 4(b). Different colors correspond to the average value of the change of energy on a given energy level due to scattering. The average change is positive in the right well, and negative in the left well. In the upper domain the average energy change is zero. There are also regular domains at the very center of the two bottom cells, where particles do not intersect the resonance at all.

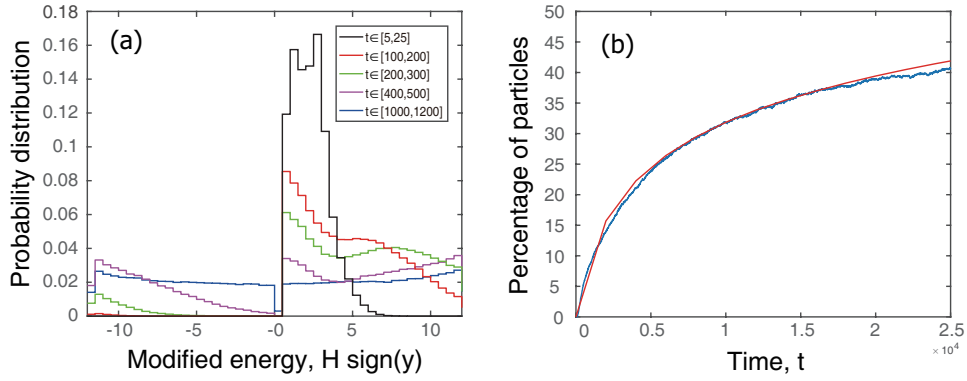

FIG. 5. Evolution of a particle ensemble. (a): Histograms of the PDF for different values of time. From the initial distribution in the right well (black curve), over the top, to the left well. Note, that the axis is the energy H multiplied by sign(y). At $t \approx 100$, the particles are in the right well; at $t \approx 250$ particles fill the right well and start coming into the left well; at $t \approx 500$ particles fill the left well; at $t \approx 1000$ particles essentially uniformly fill both bottom wells. (b): The percentage of particles in the upper domain above $H = 15$. The red curve is obtained by solving PDE (5) for the PDF, and the blue curve is the aggregation of explicit simulation of $20,000$ particle governed by (1).

To describe mixing between the wells and the evolution of the ensemble of particles, we introduced a Probability Distribution Function (PDF). We performed a set of numerical simulations of $20,000$ particles that were originally localized at $H = 1$ in the right well, Fig. 5(a). Particles start as a relatively narrow distribution in the right well (black curve). Scattering on resonances cause the maximum of the curve to move to the right, while the distributions become wider. When particles arrive to the top of the hill between the wells (red curve), they immediately start dropping into the left well. After a characteristic time of one full slow period, the distribution becomes essentially uniform in the two bottom wells. There are two characteristic times of the system: the period of the cell, T_C, and the characteristic time of mixing, T_M. Period T_C is defined by the rate of drift $\langle \Delta H \rangle$ and the probability of trapping, $\Pi(H)$ computed at $H = H_{lr}$. Rate of mixing T_M is defined by the second moment of $\langle \Delta H \rangle$:

$$T_C \approx 2 \int_{H_{min}}^{H_C} T(H) \frac{dH}{\langle \Delta H \rangle} + \frac{1}{\Pi(H = H_{lr})} \int_{H_{min}}^{H_{lr}} T(H) \frac{dH}{\langle \Delta H \rangle}, \quad T_M \approx 2\, T(H) \frac{(H_C - H_{min})^2}{\left\langle (\Delta H)^2 \right\rangle} \tag{4}$$

where $T(H)$ is the period of motion on the (y, p) phase plane. The first term in T_C (approximately equal to 850) is a time over which the drift takes a particle from the bottom of the right well to the bottom of the left well. The second term (approximately equal to 1000) is defined as the time a particle spends near the bottom of the left well before it gets into the L-R trapping.

The drift and diffusive spreading described above create an essentially uniform mixing in the two bottom wells. Beyond that, over a significantly longer time scale, more and more particles diffuse higher into the upper domain, further away from the separatrix. As a result, they stay there longer, creating a significant population. To estimate the rate of transfer into the upper well, we can use the diffusion-type evolution equation for $\Psi(H, t)$. Numerical simulations indicate that the characteristic time scales of the diffusion into the upper domain is much longer than the time-scale of the uniformization in the bottom wells. Thus we can assume that particles are uniformly distributed over the two bottom wells. Trapping into resonance does not occur in the upper domain, and dynamics is determined entirely by scattering on resonance. Scattering on resonance cause a random walk in terms of H. In the upper domain, $\langle \Delta H \rangle = 0$. For any random walk, the diffusion coefficient is equal to one half of the second moment of the corresponding distribution of the magnitude of a single step. On each period, there are two resonance crossings with the same statistical properties. We obtain $D(H) = \left\langle (\Delta H)^2 \right\rangle$, and the evolution of $\Psi(H, t)$ can be described by a diffusion-type equation PDE:

$$\frac{\partial \Psi}{\partial t} T(H) = \frac{\partial}{\partial H} \left(D(H) \frac{\partial \Psi}{\partial H} \right). \tag{5}$$

The values of $D = D(H)$ are much larger for $H_C < H < H_C + u^2/2 = 13$, where trajectories intersect the resonance four times on a period (including two crossings near $y = 0$), than for $H > H_C + u^2/2$ (two resonance crossings, away from $y = 0$), see Fig 1(b). Essentially, we can set $D(H < H_C + u^2/2) = \infty$ (uniform mixing) and explicitly study the domain $H > H_C + u^2/2$ only. We compared the predictions of (5) with results of explicit simulation of $20,000$

particle governed by (1). Figure 5(b) presents the amount of particles in the upper domain above $H = 15$. One can see that the PDF-based description describes the leaking of particle into the upper domain.

In conclusion, we considered a motion of charged plasma particles in a nonuniform background magnetic field in the presence of an electrostatic wave. We proposed a setting where the nonlinear resonance create a large scale convection cell in the phase space. We showed that a combination of the energy drift due to scattering at resonance and trapping (capture) at resonance creates a regular energy drift, while scattering at resonance create the energy diffusion and mixing. We estimated a characteristic period of the cell and characteristic time of mixing.

Fan Wu is fully supported by the National Natural Science Fund of China (Award No. 11702331). This material is based in part upon work supported by the National Science Foundation under Award No. CMMI-1740777 (D.V.).

[1] B. Eliasson, P. K. Shukla, Formation and dynamics of coherent structures involving phase-space vortices in plasmas, Phys.Rep. 422, 225–290 (2006).
[2] P. Guio, S. Børve, L. K. S. Daldorff, J. P. Lynov, P. Michelsen, H. L. Pécseli, J. J. Rasmussen, K. Saeki, and J. Trulsen, Phase space vortices in collisionless plasmas, Nonlinear Processes in Geophysics 10, 75–86 (2003).
[3] F. Zonca, L. Chen, S. Briguglio, G. Fogaccia, G. Vlad, and X. Wang, Nonlinear dynamics of phase space zonal structures and energetic particle physics in fusion plasmas, New Journal of Physics 17, 013052 (2015).
[4] O. Piro, M. Feingold, Diffusion in three-dimensional Liouvillian maps, Phys. Rev. Lett. 61, 1799–1802 (1988).
[5] M. Feingold, L. Kadanoff, and O. Piro, Passive scalars, 3-dimensional volume-preserving maps, and chaos, J. of Stat. Phys. 50, 529–565 (1988).
[6] J. Cartwright, M. Feingold, and O. Piro, Global diffusion in a realistic three-dimensional time-dependent nonturbulent fluid flow, Phys. Rev. Lett. 75, 3669–3672 (1995).
[7] H. Aref et al., Frontiers of chaotic advection, Reviews of Modern Physics 89, 025007 (2017).
[8] J. M. Albert, X. Tao, and J. Bortnik, Aspects of Nonlinear Wave-Particle Interactions, in: D. Summers, I. U. Mann, D. N. Baker, and M. Schulz (Eds.), Dynamics of the Earth's Radiation Belts and Inner Magnetosphere, American Geophysical Union, 2013.
[9] Y. Omura, D. Nunn, and D. Summers, Generation Processes of Whistler Mode Chorus Emissions: Current Status of Nonlinear Wave Growth Theory, in: D. Summers, I. U. Mann, D. N. Baker, and M. Schulz (Eds.), Dynamics of the Earth's Radiation Belts and Inner Magnetosphere, American Geophysical Union, (2013).
[10] N. M. Kroll, P. L. Morton, and M. N. Rosenbluth, Free-electron lasers with variable parameter wigglers, IEEE Journal of Quantum Electronics 17, 1436–1468 (1981).
[11] A. Osmane, D. L. Turner, L. B. Wilson, A. P. Dimmock, and T. I. Pulkkinen, Subcritical Growth of Electron Phase-space Holes in Planetary Radiation Belts, Astrophys. J. 846, 83 (2017).
[12] A. V. Artemyev, A. I. Neishtadt, D. L. Vainchtein, A. A. Vasiliev, I. Y. Vasko, and L. M. Zelenyi, Trapping (capture) into resonance and scattering on resonance: Summary of results for space plasma systems, Communications in Nonlinear Science and Numerical Simulations 65, 111–160 (2018).
[13] T. O'Neil, Collisionless Damping of Nonlinear Plasma Oscillations, Physics of Fluids 8, 2255–2262 (1965).
[14] R. K. Mazitov, Damping of plasma waves, Journal of Applied Mechanics and Technical Physics 6, 22–25 (1965).
[15] F. Valentini, P. Veltri, and A. Mangeney, Magnetic-field effects on nonlinear electrostatic-wave Landau damping, Phys. Rev. E 71, 016402 (2005).
[16] I. Y. Dodin, N. J. Fisch, Adiabatic nonlinear waves with trapped particles. III. Wave dynamics, Physics of Plasmas 19 (1), 012104 (2012).
[17] D. Bénisti, Nonlocal adiabatic theory. I. The action distribution function, Physics of Plasmas 24 (9), 092120 (2017).
[18] X. Tao, F. Zonca, and L. Chen, Identify the nonlinear wave-particle interaction regime in rising tone chorus generation, Geophys. Res. Lett. 44 (8), 3441–3446 (2017).
[19] A. Neishtadt, A. Vasiliev, and A. Artemyev, Resonance-induced surfatron acceleration of a relativistic particle, Moscow Mathematical Journal 11 (3), 531–545 (2011).
[20] A. P. Itin, A. I. Neishtadt, and A. A. Vasiliev, Captures into resonance and scattering on resonance in dynamics of a charged relativistic particle in magnetic field and electrostatic wave, Physica D 141, 281–296 (2000).
[21] A. I. Neishtadt, On Adiabatic Invariance in Two-Frequency Systems, in Hamiltonian Systems with Three or More Degrees of Freedom, ed. Simo C., NATO ASI Series C. Dordrecht: Kluwer Acad. Publ. 533, 193–213 (1999).
[22] A. Neishtadt, Passage through a separatrix in a resonance problem with a slowly-varying parameter, Journal of Applied Mathematics and Mechanics 39, 594–605 (1975).
[23] V. I. Arnold, V. V. Kozlov, and A. I. Neishtadt, Mathematical Aspects of Classical and Celestial Mechanics, 3rd Edition, Dynamical Systems III. Encyclopedia of Mathematical Sciences, Springer-Verlag, New York, 2006.
[24] A. V. Artemyev, A. A. Vasiliev, D. Mourenas, A. I. Neishtadt, O. V. Agapitov, and V. Krasnoselskikh, Probability of relativistic electron trapping by parallel and oblique whistler-mode waves in Earth's radiation belts, Physics of Plasmas 22 (11), 112903 (2015).
[25] A. V. Artemyev, A. I. Neishtadt, A. A. Vasiliev, and D. Mourenas, Probabilistic approach to nonlinear wave-particle resonant interaction, Phys. Rev. E 95 (2), 023204 (2017).